Check for updates

Received: 5 September 2024 | Revised: 22 August 2025 | Accepted: 25 August 2025

DOI: 10.1111/bph.70204

RESEARCH ARTICLE

Identification of prokineticin-2 as potential pharmacodynamic biomarker for overcoming doxorubicin resistance in multicellular breast cancer spheroids

Martina Vincenzi[1,2] | Amin Kremic[1] | Nathalie N. Tscheiller[1] | Po-Yen Hsu[1,3] | Michael W. Y. Chan[3] | Roberta Lattanzi[2] | Canan G. Nebigil[1]

[1]Regenerative Nanomedicine (UMR 1260), INSERM, University of Strasbourg, Center of Research in Biomedicine of Strasbourg, Strasbourg, France

[2]Department of Physiology and Pharmacology 'Vittorio Erspamer', Sapienza University of Rome, Rome, Italy

[3]Department of Biomedical Sciences, National Chung Cheng University, Chiayi, Taiwan

Correspondence
Canan G. Nebigil, Regenerative Nanomedicine (UMR 1260), INSERM, University of Strasbourg, Center of Research in Biomedicine of Strasbourg, Strasbourg, France.
Email: nebigil@unistra.fr

Funding information
Sapienza University of Rome doctoral fellowship; Fondation de France, Grant/Award Numbers: R20085MM, R023044MM; Agence Nationale de la Recherche grants, Grant/Award Number: ANR 16-ECVD-0005-09; Italian Society of Pharmacology (SIF) fellowship

Background and purpose: Despite advances in immunotherapy, doxorubicin (Dox) chemotherapy is still the irreplaceable first-line therapy for solid tumours such as breast cancer. However, chemotherapy resistance is the major limiting factor, requiring the use of high doses of Dox to achieve the anti-tumour actions, often leading to severe side effects. Unravelling the mechanisms behind chemoresistance and identifying potential biomarkers for mitigating this resistance could enhance current treatment strategies and improve patient outcomes.

Experimental approach: We developed human 3D breast cancer spheroids (HBCSs) as a model that closely mimics in vivo tumour structure and microenvironment. Given that hypoxia and elevated levels of the angiogenic cytokine, prokineticin-2 (PK2), are associated with chemoresistance to antiangiogenic therapy, we explored the effect of a hypoxia-inducible factor (HIF-1α) inhibitor on viability defect in HBCSs and the levels of PK2 in the conditioned medium following Dox treatment. We also assessed levels of HIF-1α, active caspase-3, TUNEL and reactive oxygen species (ROS), and CD73 enzymatic activity in HBCSs.

Key results: Results showed that HIF-1α inhibitor increased viability defect in the Dox-resistant HBCSs. Interestingly, at higher Dox concentrations, chemoresistance was mitigated independently of HIF-1α and promoted apoptosis and ROS accumulation, which were correlated with PK2 release.

Conclusions and implications: Our findings provide the first evidence that PK2 may serve as a predictive pharmacodynamic marker, offering a potential strategy to overcome drug resistance in targeted cancer therapy.

KEYWORDS
breast cancer, chemoresistance, doxorubicin, hypoxia, prokineticin 2, reactive oxygen species

Abbreviations: Bcl-2, B-cell lymphoma 2 (an anti-apoptotic protein); CD73, Cluster of differentiation 73 (also known as ecto-5′-nucleotidase); DAPI, 4′,6-Diamidino-2-Phenylindole (a fluorescent stain that binds strongly to DNA); DHR-123, Dihydrorhodamine 123 (a fluorescent probe used to detect reactive oxygen species); Cas3, Caspase-3; Dox, Doxorubicin; EC, Endothelial cell; FB, Fibroblast; GFP, Green fluorescent protein; GLUT-1, Glucose transporter 1; GUSB, Beta-glucuronidase; HBCSs, Human breast cancer spheroids; HIF-1α, Hypoxia-inducible factor 1-alpha; HIF-1β, Hypoxia-Inducible Factor 1-beta; KC7F2, N,N′-(2,5-Dichlorosulfonyl) cystamine an inhibitor of HIF-1α; OTC, Optimal cutting temperature compound; p53, Tumour protein p53 (also known as TP53); PK2, Prokineticin-2; TUNEL, Terminal deoxynucleotidyl transferase dUTP nick-end labelling; ULA, Ultra-low attachment.

This is an open access article under the terms of the Creative Commons Attribution License, which permits use, distribution and reproduction in any medium, provided the original work is properly cited.
© 2025 The Author(s). *British Journal of Pharmacology* published by John Wiley & Sons Ltd on behalf of British Pharmacological Society.

1 | INTRODUCTION

Over the past decade, the burden of non-communicable diseases, including cancers, has increased because of population ageing, urbanisation and physical inactivity. Cancer is now the second leading cause of death worldwide. According to the GLOBOCAN report, solid tumours such as breast cancers are the most prevalent, accounting for 11.7% of all new cancer cases worldwide (Sung et al., 2021). Despite recent advances in therapeutic strategies, cytotoxic agents such as anthracyclines remain common first-line treatments for these solid tumours (Nebigil & Désaubry, 2018). In fact, doxorubicin (Dox), the prominent anthracycline, is currently considered as the most effective combination adjuvant drug for treating breast cancer, particularly triple-negative breast cancer (Hernandez-Aya & Gonzalez-Angulo, 2013; Shi et al., 2018). Dox induces cell death through various intracellular interactions, including the generation of reactive oxygen species (ROS) and DNA-double-strand breaks, inhibition of **topoisomerase II** and histone eviction (Kciuk et al., 2023). However, Dox has been found to promote resistance by supporting tumour growth and metastasis in 20–30% of patients (Chen et al., 2023; Lovitt et al., 2018; Pan et al., 2021).

Increasing Dox concentrations to counteract chemoresistance and achieve effective therapeutic outcomes can result in undesirable side effects such as cardiotoxicity, which worsen clinical outcomes (Dulf et al., 2023). Therefore, understanding the mechanisms underlying the development of chemoresistance is crucial to improve patient prognosis and survival through optimised therapeutic strategies.

Resistance to Dox can arise from either acquired or intrinsic mechanisms. Some of the investigated mechanisms include defects in tumour suppressor p53 (Aas et al., 1996), activation of the mitogen-activated protein kinase (**MAPK)**/extracellular-signal-regulated kinase (**ERK**) and phosphoinositide 3-kinase (PI3K)/**Akt** pathway (Christowitz et al., 2019), the overexpression of efflux pumps such as **P-glycoprotein** (Mechetner et al., 1998), the epithelial–mesenchymal transition process (Ponnusamy et al., 2017) and the development of hypoxia (Doublier et al., 2012; Fourie et al., 2022).

Hypoxia is a key factor in reducing the sensitivity of solid tumours to chemotherapy, radiotherapy and immunotherapy because of the hypoxia-inducible factor-1 (HIF-1) complex (Fan et al., 2023). As a central component of hypoxic adaptation, this complex promotes the transcription of genes involved in tumour growth and vascularisation, stromal cell recruitment, extracellular matrix remodelling, cell motility and metastasis (Semenza, 2016). As a result, hypoxia is considered the driving force behind chemoresistance in solid tumours (Bouleftour et al., 2021). Numerous preclinical studies have identified the HIF-1 complex as potential tumour-specific target for sensitising cancer cells to chemotherapeutic agents (Doublier et al., 2012; Li et al., 2006; Song et al., 2006; Zhou et al., 2023). Additionally, alternative angiogenic pathways have been implicated in the development of resistance to certain chemotherapeutics such as anti-VEGF treatments in cancers (Haibe et al., 2020). The up-regulation of proangiogenic cytokine, **prokineticin 2** (PK2), has been shown to mediate myeloid cell-dependent tumour angiogenesis (Shojaei et al., 2007) and is associated with refractoriness to anti-VEGF therapy (Shojaei et al., 2009). Indeed, PK2 via its receptor (**PKR_1**) promotes angiogenesis in cardiac endothelial cells (ECs) and the anti-oxidative pathway in response to Dox-mediated accumulation of ROS in cardiomyocytes (Gasser et al., 2019). Although, Dox is a very potent cytotoxic agent in cardiomyocytes, cardiac, endothelial, progenitor cells (Gasser et al., 2019) and the cancer EC system (Zhang et al., 2002), the potential association between PK2 production in cancer and development of Dox-mediated resistance has not yet been studied.

However, much of our current understanding of cancer biology is derived from in vitro studies on two-dimensional (2D) cultures. Previous research has demonstrated that Dox can induce apoptosis and the development of resistance in 2D cultures of solid cancers, including breast cancer MDAMB231 and MCF7 cell lines (Badinloo & Esmaeili-Mahani, 2014; Wang et al., 2004; Yeh et al., 2004). However, the interaction between cancer cells and their surrounding stromal cells, such as fibroblasts, immune and ECs, have been shown to regulate various features of tumour growth and drug resistance (Bissell & Radisky, 2001). The development of multicellular tumour spheroids has partially addressed the limitation of 2D cultures, enabling better prediction of the in vivo efficacy of various chemotherapeutic agents (Mehta et al., 2012).

Building on this evidence, we used multicellular spheroids, composed of cancer cells, fibroblasts and ECs, as a model for breast cancer. We treated these 3D spheroids with varying concentrations of

What is already known?

- Triple negative breast cancer patients may develop drug resistance after exposure to neoadjuvant chemotherapy
- They may eventually die from tumour recurrence or metastasis.

What does this study add?

- We identify mechanisms for reversal of doxorubicin-induced chemotherapy resistance and establish a pharmacodynamic biomarker, prokineticin-2.
- ROS-dependent DNA damage can help overcome doxorubicin resistance in breast cancer spheroids.

What is the clinical significance?

- These findings support the clinical potential of prokineticin-2 as a biomarker for overcoming chemoresistance.
- This suggests more effective therapeutic strategies and improving patient survival in breast cancer.

14765381, 0, Downloaded from https://bpspubs.onlinelibrary.wiley.com/doi/10.1111/bph.70204 by Martina Vincenzi - University Di Roma La Sapienza , Wiley Online Library on [16/10/2025]. See the Terms and Conditions (https://onlinelibrary.wiley.com/terms-and-conditions) on Wiley Online Library for rules of use; OA articles are governed by the applicable Creative Commons License

Dox to assess the 3D model's ability to recapitulate the in vivo tumour response to treatment. Our goal was to study the mechanism involved in overcoming hypoxia-mediated chemoresistance and to identify potential biomarkers of the counteracting response to the resistance.

2 | METHODS

2.1 | Materials

The human breast cancer cell line, MDAMB231 (RRID: CVCL_0062), and its complete medium were obtained from the Integrated Structural Biology Platform of the IGBMC (Strasbourg, France). Green fluorescent protein (GFP)-expressing human umbilical vein ECs (PELOBiotec Cat# PB-CAP-0001GFP), human pulmonary fibroblasts (FBs, PELOBiotec Cat# PB-CH-450-0811) and the respective growth media were purchased from PELObiotech GmbH (Planegg, Germany). T75 flask was from Corning (New York, USA), whereas 96-well ultra-low attachment (ULA) plate was purchased from S-bio (Hudson, New Hampshire, USA). The CellTiter Glo 3D cell viability kit was from Promega (Madison, WI, USA). White-opaque 96-well plates (Nunc), Optimal Cutting temperature (OTC) compound, SuperFrost plus slides, DAPI (Invitrogen) and Trizol reagent were obtained from ThermoFisher Scientific (Waltham, USA). Doxorubicin hydrochloride (Dox), KC7F2, Triton X-100, bovine serum albumin (BSA), Eukitt, sucrose, $CaCl_2$, Tris-maleate buffer, AMP, Pb $(NO_3)_2$, $MnCl_2$, Dextran T250, $(NH4)_2S$ and dihydrorhodamine-123 (DHR-123) were from Sigma-Aldrich (Merck group, Darmstadt, Germany); TACS-2 TdT-DAB in situ apoptosis detection kits were from R&D Biotechne (Minneapolis, MN, USA), and fluoromount was from Ibidi GmbH (Gräfelfing, Germany). Enzyme-linked immunosorbent assay (ELISA) kits for PK2 were purchased from Cloud-clone Corp (Katy, TX, USA).

2.2 | Generation of cancer spheroids

Human breast cancer cell line, MDAMB231 (triple-negative breast cancer), kindly donated by the Integrated Structural Biology Platform of the IGBMC (Strasbourg, France), was cultured in Roswell Park Memorial Institute (RPMI) 1640 medium without HEPES with 10% fetal calf serum (FCS) and 40 μg ml^{-1} gentamycin. GFP-expressing human umbilical vein ECs and human pulmonary fibroblasts (FBs) were seated in the respective growth media. All cells were cultured separately in T75 flasks at 37°C and 5% CO_2. When 80% confluence was reached, cells were detached using diluted trypsin solution, transferred to 50 ml tubes, centrifuged at 300 × g for 5 min, resuspended in the correct medium and counted using an automated haemocytometer (Bio-Rad, Hercules, CA, USA). Maximus passage number 10 was used for ECs and FBs.

To generate breast cancer spheroids, MDAMB231 cells were cultured with FBs and ECs at a ratio of 1:2:2, in 200 μl of spheroid medium per well in a 96-well ultra-low attachment (ULA) plate. MDAMB231/FB/EC spheroid medium was prepared by mixing MDAMB231 medium with both human FB and EC growth medium in a ratio of 1:2:2 (Yakavets et al., 2020; Yu et al., 2021). Plates were kept at 37°C and 5% CO_2 and spheroid morphology were observed daily for 7 days using EVOS XL core microscope (ThermoFisher Scientific, Waltham, USA) until spheroid maturation was achieved.

2.3 | Treatments

Breast cancer spheroids were exposed to various increasing concentrations (1–3–10–30–100–300–400 μM) of Dox hydrochloride for 72 h at 37°C in a humidified incubator with 5% CO_2. The 50 μM HIF-1α translation inhibitor (KC7F2) was added simultaneously with Dox in the Dox + HIF-1α inhibitor group while fresh spheroid medium was used for the control group (Vehicle). KC7F2 was selected as a cell-permeable HIF-1α inhibitor because it selectively suppresses cellular HIF-1α, but not HIF-1β, protein synthesis without affecting HIF-1α mRNA transcription or HIF-1α protein stability, and it reduces HIF-1α-dependent pro-survival genes.

2.4 | Viability assay

The spheroid viability was determined using the CellTiter Glo 3D cell viability assay according to the manufacturer's instructions. In brief, spheroids were transferred into white-opaque 96-well plates (Nunc) with 100 μl of conditioned culture medium. An equal volume of CellTiter-Glo 3D reagent was added to each well. The plates were protected from light and shaken for 7 min to induce spheroid lysis. After, the samples were incubated at room temperature for 25 min to stabilise the bioluminescent signal and the amount of ATP was measured using a luminometer (1450 MicroBeta TriLux, PerkinElmer, USA).

2.5 | Real-time quantitative polymerase chain reaction (PCR)

Total RNA was extracted from 20 spheroids per group, using Trizol reagent, and 400 ng of RNA was reverse transcribed to cDNA using reverse transcriptase (Vazyme, Red Maple Hi-tech Industry Park, Nanjing, PRC, China). Real-time quantitative PCR (RT-PCR) was performed using the SYBR Green I real-time detection kit on a XX Detection System (Bio-Rad, Hercules, CA, USA). The relative gene expression was normalised to GUS X. The primers were listed in Table 1.

2.6 | Immunofluorescence

After treatments, spheroids were collected and embedded in Optimal Cutting temperature (OTC) compound and stored at −80°C. Spheroid sections (10 μm) were cut on a cryostat (Leica CM3050S, Germany), mounted on SuperFrost plus slides and dried at room temperature before immunolabelling.

14765381, 0, Downloaded from https://bpspubs.onlinelibrary.wiley.com/doi/10.1111/bph.70204 by Martina Vincenzi - University Di Roma La Sapienza , Wiley Online Library on [16/10/2025]. See the Terms and Conditions (https://onlinelibrary.wiley.com/terms-and-conditions) on Wiley Online Library for rules of use; OA articles are governed by the applicable Creative Commons License

TABLE 1 Primers.

Gene	Forward	Reverse
Vimentin	5′-CCACGAAGAGGAAATCCAGGAG-3′	5′-TACCATTCTTCTGCCTCCTGC-3′
GLUT1	5′-GGCCAAGAGTGTGCTAAAGAA-3′	5′-ACAGCGTTGATGCCAGACAG-3′
Bcl2	5′-GGAGGATTGTGGCCTTCTTT-3′	5′-GCCCAATACGACCAAATCCGTTGA-3′
Cas3	5′-TTAATAAAGGTATCCATGGAGAACACT-3′	5′-TTAGTGATAAAAAAGAGTTCTTTTGTGAG-3′

TABLE 2 Primary and secondary antibodies used for immunofluorescence labelling.

Antibody	Clonality	Host	Dilution	Source	Cat#	RRID
HIF-1α	Polyclonal	Rabbit	1 μg ml^{-1}	Atlas	HPA000907	AB_2666139
Active caspase 3	Polyclonal	Rabbit	1:1000	Sigma-Aldrich	C8487	AB_476884
Anti-rabbit IgG (H + L) Highly cross-adsorbed secondary antibody, Alexa Fluor™ 647	Polyclonal secondary	Donkey	5 μg ml^{-1}	Invitrogen	A-31573	AB_2536183

The pre-warmed spheroid sections were fixed in 4% paraformaldehyde (PFA) for 15 min at 4°C and washed three times with 1X PBS (10 min each). After incubation in blocking solution (containing 0.1% Triton X-100 and 1% bovine serum albumin [BSA] in 1X PBS) for 1 h at room temperature, the slides were treated overnight at 4°C with the primary antibodies (Table 2) diluted in blocking solution. All the primary antibodies solutions were maintained at −20°C and re-used maximum 2 times. The spheroid cryosections were rinsed three times (10 min each) in 1X PBS, followed by incubation in the dark with secondary antibody in 1X PBS (Table 2) for 1 h at room temperature. Secondary antibody solutions were freshly prepared for each experiment, and control experiments in the absence of the primary antibodies were performed to check the secondary antibody signal and Dox autofluorescence. After washing three times in 1X PBS (10 min each), nuclei were immunolabelled with DAPI (1:50000, in 1X PBS) and slides were mounted with Fluoromount. Images were acquired through the 10X and 63X oil immersion objective on the Zeiss Axio Imager M2 microscope at the PIC-STRA UMS38 platform (CRBS, INSERM, Strasbourg, France) and analysed offline using FIJI software (National Institutes of Health, USA).

2.7 | Enzymatic activity assay

The activity of 5′-ectonucleosidase (NT5E, also known as CD73) was assessed using the slightly modified method of Wachstein and Meisel (1957) described by Braun et al. (2000). Briefly, pre-warmed spheroid cryosections were fixed in 4% PFA for 15 min at 4°C, washed three times and incubated for 30 min at room temperature in Tris-maleate-sucrose (TMS) buffer (containing 0.25 M sucrose, 2 mM $CaCl_2$ in 50 mM Tris-maleate buffer, pH 7.4). The enzymatic reaction was performed by incubating the slides with 200 μM AMP in TMS buffer supplemented with 2 mM Pb $(NO_3)_2$, 5 mM $MnCl_2$ and 3% Dextran T250 for 2 h at room temperature. In control experiments (not shown), the substrate was omitted from the incubation solution. Nucleotide hydrolysis resulted in the precipitation of orthophosphate lead, which was visualised in situ by incubating the sections in an aqueous solution of 1% $(NH4)_2S$. Subsequently, all sections were counterstained with 1% methyl green, dehydrated in an increasing proportion of ethanol and xylene and mounted with Eukitt. Images were acquired at 10X magnification using the Zeiss Axio Imager M2 microscope at the PIC-STRA UMS38 platform (CRBS, INSERM, Strasbourg, France).

2.8 | TUNEL apoptosis assay

To analyse the apoptosis induced by Dox treatment, spheroid cryosections were stained using TACS-2 TdT-DAB In Situ Apoptosis Detection, following the manufacturer's instructions.

2.9 | ROS detection

ROS production was assessed by a spectrofluorometric measurement of rhodamine-123 (RDH-123) at 534 nm, after excitation at 505 nm (Bueb et al., 1995). Briefly, after 72 h of treatments, spheroids were starved, exposed to 5 μM dihydrorhodamine-123 (DHR-123) and incubated at 37°C for 30 min in the dark. To measure the DHR-123 relative fluorescence units, spheroids were rapidly transferred in a 96-well flat bottom black plate with fresh medium, and fluorescence was read by a Bio-rad reader (Hercules, CA, USA).

2.10 | ELISA

At the end of the Dox treatment, the spheroid-conditioned medium was collected in microtubes on ice, centrifuged at 500 × g for 5 min at 4°C to remove cell debris, transferred to new microtubes and stored at −80°C until the ELISA assay was performed. A commercial ELISA kit for PK2 based on a competitive inhibition enzyme

14765381, 0, Downloaded from https://bpspubs.onlinelibrary.wiley.com/doi/10.1111/bph.70204 by Martina Vincenzi - University Di Roma La Sapienza , Wiley Online Library on [16/10/2025]. See the Terms and Conditions (https://onlinelibrary.wiley.com/terms-and-conditions) on Wiley Online Library for rules of use; OA articles are governed by the applicable Creative Commons License

immunoassay technique was used to quantify the release of PK2 in the spheroid-conditioned medium and was performed according to the manufacturer's instructions.

2.11 | Statistical methods and experimental rigour

Experimental design and analysis adhere to the *British Journal of Pharmacology* (*BJP*) guidelines on preclinical pharmacology research (Curtis et al., 2025). Group sizes (n ≥ 5 biological replicates per condition for statistical analysis) were calculated a priori using G*Power 3.1.9.6, with $\alpha = 0.05$, power = 0.80, effect sizes based on Saitoh and Nagase (2018), and estimated outcome variability. Experimental units were randomly assigned to groups using block randomisation, and investigators were blinded to group assignments, phenotypes and treatments. Data are presented as individual values with mean ± SEM. All data were acquired from at least 3–5 independent experiments with technical replicates (≥3–20 spheroids per experiment). Normality was assessed by the Shapiro–Wilk test. Statistical analysis was carried out only where the number of independent experiments was 5 or more. For experiments where n<5, statistical analysis was not carried out and results should be regarded as preliminary. Where data were approximately normally distributed, one- or two-way analysis of variance (ANOVA) followed by Bonferroni's post hoc tests was applied for multiple comparisons; when required, non-parametric alternatives were used. Post-hoc tests were run only if F achieved P<0.05 and there was no significant variance inhomogeneity. Statistical significance was defined as $P < 0.05$. ELISA and viability data were normalised to the control baseline to reduce technical variability.

2.12 | Nomenclature of targets and ligands

Key protein targets and ligands in this article are hyperlinked to corresponding entries in http://www.guidetopharmacology.org, and are permanently archived in the Concise Guide to PHARMACOLOGY 2023/2024 (Alexander, Christopoulos, Davenport, Kelly, Mathie, Peters, Veale, Armstrong, Faccenda, Harding, Davies, et al., 2023; Alexander, Fabbro, Kelly, Mathie, Peters, Veale, Armstrong, Faccenda, Harding, Davies, Amarosi, et al., 2023; Alexander, Fabbro, Kelly, Mathie, Peters, Veale, Armstrong, Faccenda, Harding, Davies, Annett, et al., 2023; Alexander, Kelly, Mathie, Peters, Veale, Armstrong, Buneman, Faccenda, Harding, Spedding, Cidlowski, et al., 2023).

3 | RESULTS

3.1 | Evaluation of Dox efficacy in the 3D breast cancer spheroids

The experimental scheme is illustrated in Figure 1a. MDAMB231 cells, ECs and FBs were co-cultured to mimic in vivo tumour organisation

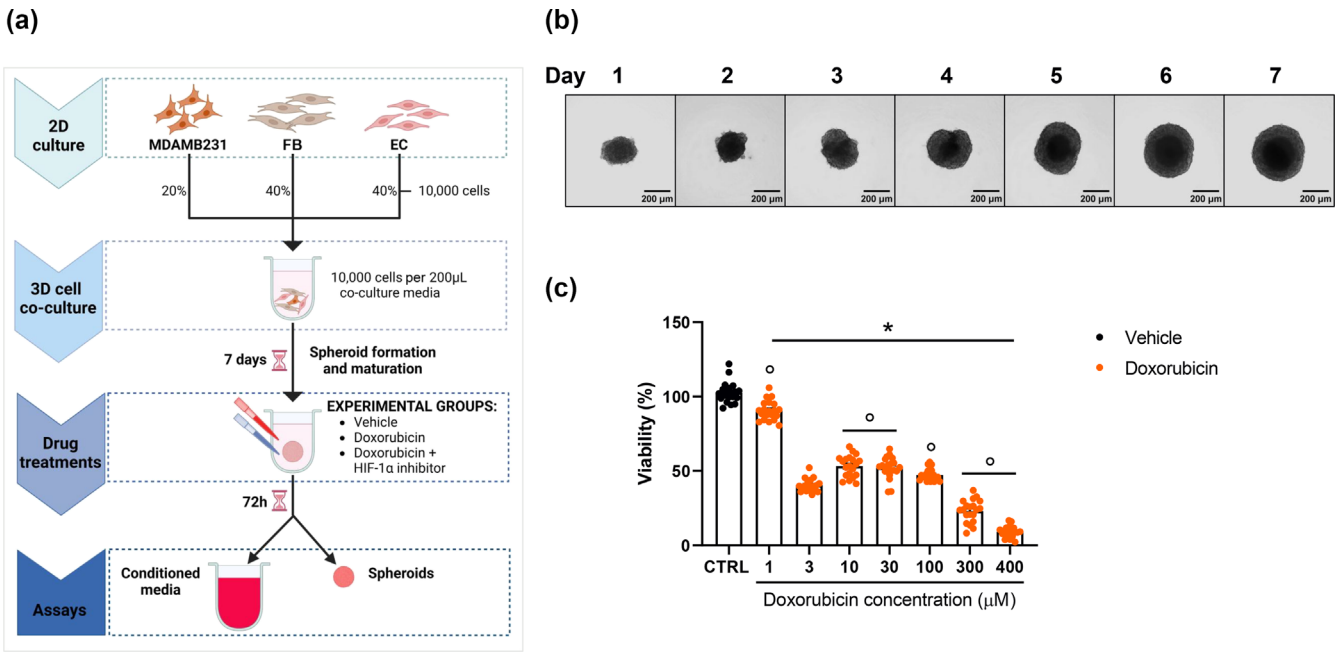

FIGURE 1 Effect of Doxorubicin (Dox) on viability of breast cancer spheroids. (a) Experimental outline. (b) Daily images showing spheroid growth. Scale bar = 200 µM. (c) Results of the CellTiter-Glo 3D cell viability assay, which measures ATP content as an indicator of viable cells, in MDAMB231/FB/EC spheroids after 72h of Dox exposure. Data were analysed using one-way ANOVA followed by Bonferroni's multiple comparison post hoc test. Results are expressed as percentage ± SEM of four spheroids per group from $n = 5$ independent experimental settings. Statistical significance was set at *$P < 0.05$ versus vehicle group (control, CTRL) and $P < 0.05$ versus 3 µM Dox-treated spheroids. ($P < 0.0001$, all Dox-treated groups vs vehicle group; $P < 0.0001$, 1–10 µM–30 µM–300 µM and 400 µM Dox-treated spheroids vs 3 µM Dox-treated samples; $P = 0.0031$, 100 µM Dox-treated spheroids vs 3 µM Dox-treated samples). EC, Endothelial cell; FB, Fibroblast.

14765381, 0, Downloaded from https://bpspubs.onlinelibrary.wiley.com/doi/10.1111/bph.70204 by Martina Vincenzi - University Di Roma La Sapienza , Wiley Online Library on [16/10/2025]. See the Terms and Conditions (https://onlinelibrary.wiley.com/terms-and-conditions) on Wiley Online Library for rules of use; OA articles are governed by the applicable Creative Commons License

and replicate the tumour microenvironment. Spheroid growth was monitored daily, as shown in Figure 1b. To determine the response of our heterocellular breast cancer spheroids (HBCSs) to Dox treatment, we assessed their viability after 72 h of exposure to increasing concentrations of Dox (1–3–10–30–100–300–400 μM). A statistically significant reduction in spheroid viability was observed at all tested Dox concentrations (Figure 1c). A concentration of 1 μM Dox caused a modest reduction (approximately 10%) in spheroid viability, while 3 μM Dox led to a 60% decrease in spheroid survival compared to untreated controls. Interestingly, Dox concentrations between 10 and 100 μM resulted in less pronounced viability defects than 3 μM Dox, suggesting the emergence of development of partial chemoresistance. This reduced sensitivity was significantly overcome at higher Dox concentrations (300 and 400 μM). Thus, our 3D model provides a more accurate representation of breast cancer physiology and enables the investigation of Dox cytotoxicity.

3.2 | Doxorubicin-induced hypoxia promotes resistance in 3D spheroid breast cancer model

The development of chemoresistance can be either constitutive or acquired, involving various mechanisms (Mattioli et al., 2023). It is widely accepted that hypoxia drastically reduces chemosensitivity in a

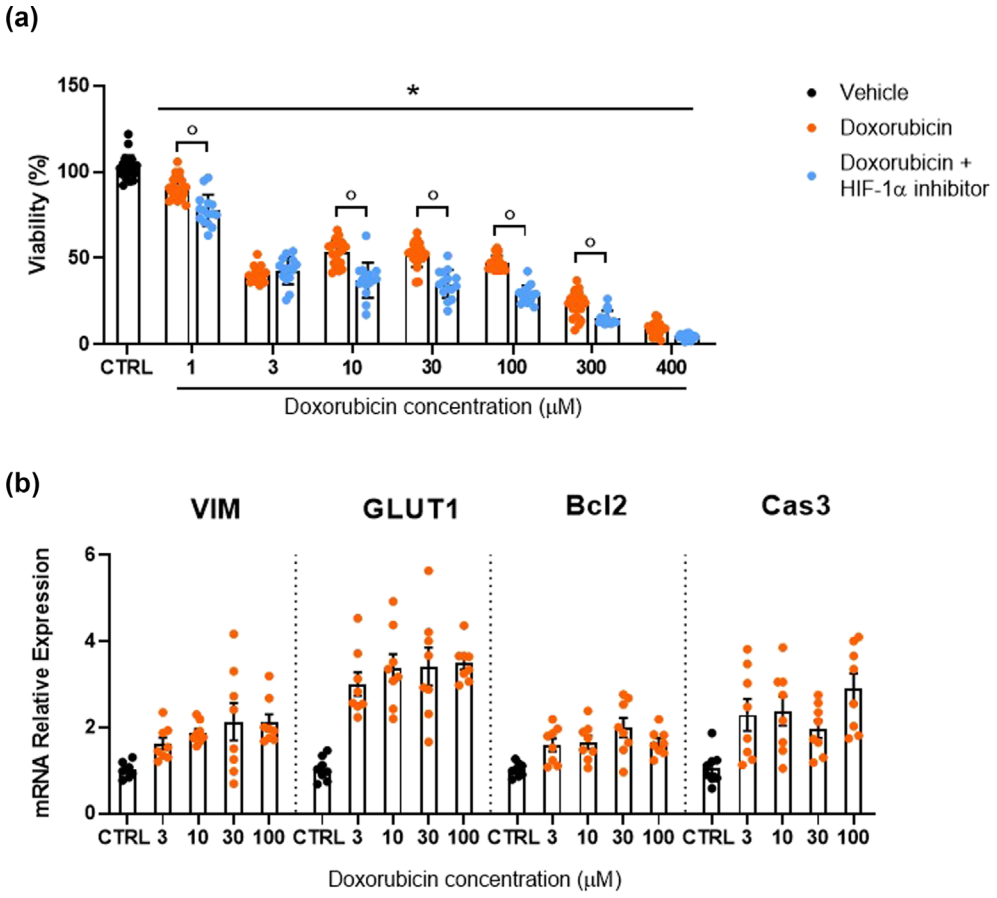

FIGURE 2 Counteracting the Doxorubicin (Dox)-mediated chemoresistance by a HIF-1α inhibitor in breast cancer spheroids. (a) Results of CellTiter-Glo 3D cell viability assay in MDAMB231/FB/EC spheroids after 72 h of Dox exposure in the presence and absence of a HIF-1α inhibitor. Data were analysed by one-way ANOVA or 2-way ANOVA followed by Bonferroni's Multiple Comparison Test. Results are expressed as percentage ± SEM of four spheroids per group and three spheroids per group from five independent experimental settings for Dox and Dox + HIF-1α inhibitor treatment, respectively. Statistical significance was set at $^*P < 0.05$ for Dox + HIF-1α inhibitor groups versus vehicle (control, CTRL) and $P < 0.05$ for Dox + HIF-1α inhibitor groups versus Dox-treated spheroids, comparing same Dox concentrations. ($P < 0.0001$, all Dox + HIF-1α inhibitor groups vs vehicle; $P < 0.0001$, 1 μM Dox + HIF-1α inhibitor vs 1 μM Dox-treated spheroids; $P < 0.0001$ for 10 μM Dox + HIF-1α inhibitor vs 10 μM Dox-treated spheroids; $P < 0.0001$, 30 μM Dox + HIF-1α inhibitor vs 30 μM Dox-treated spheroids; $P < 0.0001$, 100 μM Dox + HIF-1α inhibitor vs 100 μM Dox-treated spheroids; $P = 0.0057$, 300 μM Dox + HIF-1α inhibitor vs 300 μM Dox-treated spheroids). (b) Relative mRNA expression levels of HIF-1α-regulated genes such as Vimentin, GLUT1, Bcl2 and Caspase-3 (Cas3) were assessed by RT-PCR in pooled HBCSs. Spheroids were treated with increasing concentrations of Dox (3, 10, 30 and 100 μM), and gene expression was normalised to vehicle-treated controls. Each dot in the scatter plots represents the average of technical duplicates ± SEM from four independent experiments with technical replicates (20 spheroids per condition). Vimentin expression increased in a dose-dependent manner at higher Dox concentrations (from 10 to 100 μM); GLUT1 mRNA levels were consistently elevated across all Dox-treated groups; Bcl2 expression showed a progressive increase with rising Dox doses (from 3 up to 100 μM) while Cas3 levels were enhanced at low (3 and 10 μM) and high (100 μM) Dox concentrations, with no apparent change after 30 μM Dox treatment. EC, Endothelial cell; FB, Fibroblast

14765381, 0, Downloaded from https://bpspubs.onlinelibrary.wiley.com/doi/10.1111/bph.70204 by Martina Vincenzi - University Di Roma La Sapienza , Wiley Online Library on [16/10/2025]. See the Terms and Conditions (https://onlinelibrary.wiley.com/terms-and-conditions) on Wiley Online Library for rules of use; OA articles are governed by the applicable Creative Commons License

variety of tumour cells (Song et al., 2006; Wartenberg et al., 2003). Additionally, chemotherapeutic drugs such as Dox can induce the expression of HIF-1α in normoxic 2D tumour cells, thereby limiting their own effectiveness (Cao et al., 2013). To investigate whether the resistance observed in our 3D model might be mediated by Dox-induced hypoxia, we examined the effect of blocking HIF-1α translation with the inhibitor KC7F2 on the viability of Dox-treated spheroids.

In the presence of KC7F2, 10, 30 and 100 μM Dox significantly further decreased viability by 29.7%, 33.5% and 39.3%, respectively. Additionally, inhibition of HIF-1α resulted in a 35.4% reduction in viability in spheroids treated with 300 μM Dox, without significantly affecting the survival of those treated with 3 or 400 μM Dox (Figure 2a).

Furthermore, HIF-1α-targeted prosurvival genes, including the invasion marker vimentin (VIM) (Zhao et al., 2024), the metabolic marker glucose transporter-1 (**GLUT1**) (Liu et al., 2022) and the anti-apoptotic marker **Bcl2** (McAleese et al., 2021), were up-regulated in HBCSs treated with Dox at concentrations ranging from 10 to 100 μM, confirming HIF-1α elevation during hypoxia (Figure 2b). Interestingly, Caspase-3 expression was markedly elevated under these hypoxic conditions, indicating an impaired balance between apoptotic and anti-apoptotic gene regulation.

These findings suggest that exposure of cancer spheroids to Dox at concentrations between 10 μM to 100 μM promotes a hypoxia-mediated HIF-1α-dependent mechanism of chemoresistance. This resistance was alleviated by inhibiting HIF-1α, which sensitised the cancer spheroids to Dox's cytotoxic effects.

3.3 | Dox in high concentrations promotes sustained HIF-1α levels in breast cancer spheroids

To determine whether spheroids remained in a hypoxic state after treatment with high concentrations of Dox (100, 300 and 400 μM), we evaluated HIF-1α protein levels by immunostaining spheroid cryosections with a HIF-1α antibody (pink), while DAPI (blue) was used to label the nuclei (Figure 3a). Surprisingly, a dose-dependent increase in HIF-1α protein expression was observed in MDAMB231/FB/EC spheroids treated with high concentrations of Dox compared to untreated controls (vehicle group) (Figure 3b).

To further evaluate whether downstream pathway of HIF-1α was affected, we measured CD73 activity, as an alternative to evaluating HIF-1α-regulated gene expression via RT-PCR, which was influenced by Dox toxicity within this dose range. After translocating to the nucleus, HIF-1α enhances the transcription and activity of various target genes, including CD73 (Lee et al., 2019), a purinergic ectoenzyme, degrading ATP into adenosine (Synnestvedt et al., 2002). Our findings revealed that CD73 activity in cryosections of breast cancer spheroids increased in a concentration-dependent manner after 72 h of exposure to high Dox concentrations. This was indicated by intensified dark staining in MDAMB231/FB/EC spheroids compared to untreated controls (Figure 3c).

Our data suggest that high concentrations of Dox counteract resistance at increased hypoxia and the HIF-1α-dependent chemoresistance pathway in cancer spheroids. We hypothesised that high concentrations of Dox may activate multiple cytotoxic pathways to overcome chemoresistance, albeit at the cost of elevated HIF-1α levels.

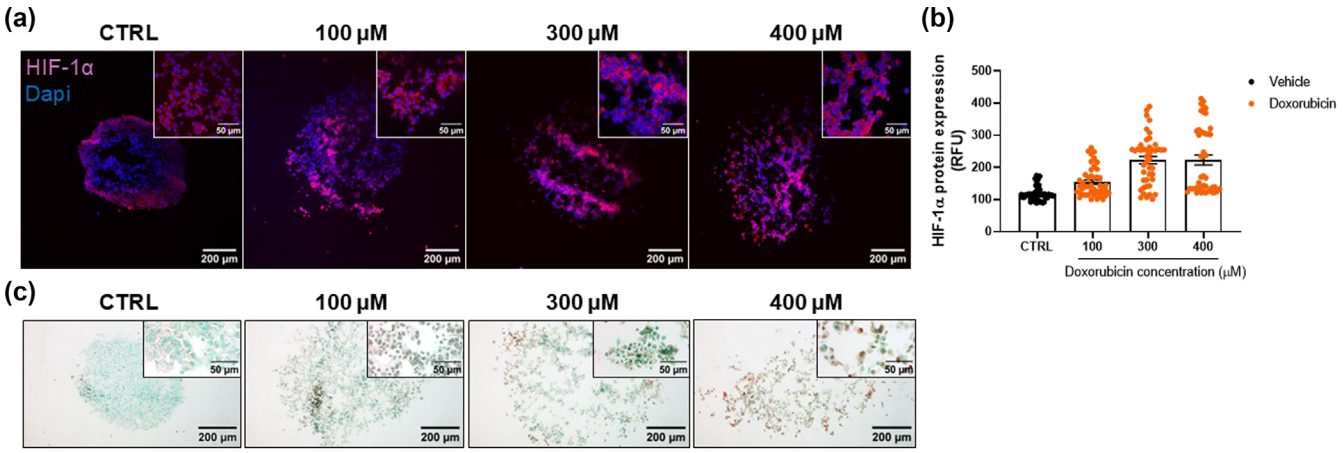

FIGURE 3 Hypoxia-mediated pathway in Doxorubicin (Dox) chemoresistance in breast cancer spheroids. (a) Representative images of HIF-1α staining (pink) in cryosectioned MDAMB231/FB/EC spheroids. Enlarged areas are shown in the inserts within the merged images. Scale bars: 200 and 50 μm. (b) Relative quantification of HIF-1α protein expression. Following Dox treatment, a notable increase of HIF-1α protein expression was detected (29.36%, 87.42% and 86.83% in 100, 300 and 400 μM Dox-treated HBCSs vs untreated controls, respectively). (c) Representative images showing the histochemical localisation of CD73 enzymatic activity in breast cancer spheroid cryosections, counterstained with 1% methyl green ($n = 3$ independent experimental settings, three spheroids per group for each experiment). The red/brown signal indicates active ADP hydrolysis, used as the reaction substrate, and is not attributed to specific cellular elements. Enlarged areas are shown in the inserts within the merged images. Scale bars: 200 and 50 μm. CTRL, control; EC, Endothelial cell; FB, Fibroblast

14765381, 0, Downloaded from https://bpspubs.onlinelibrary.wiley.com/doi/10.1111/bph.70204 by Martina Vincenzi - University Di Roma La Sapienza , Wiley Online Library on [16/10/2025]. See the Terms and Conditions (https://onlinelibrary.wiley.com/terms-and-conditions) on Wiley Online Library for rules of use; OA articles are governed by the applicable Creative Commons License

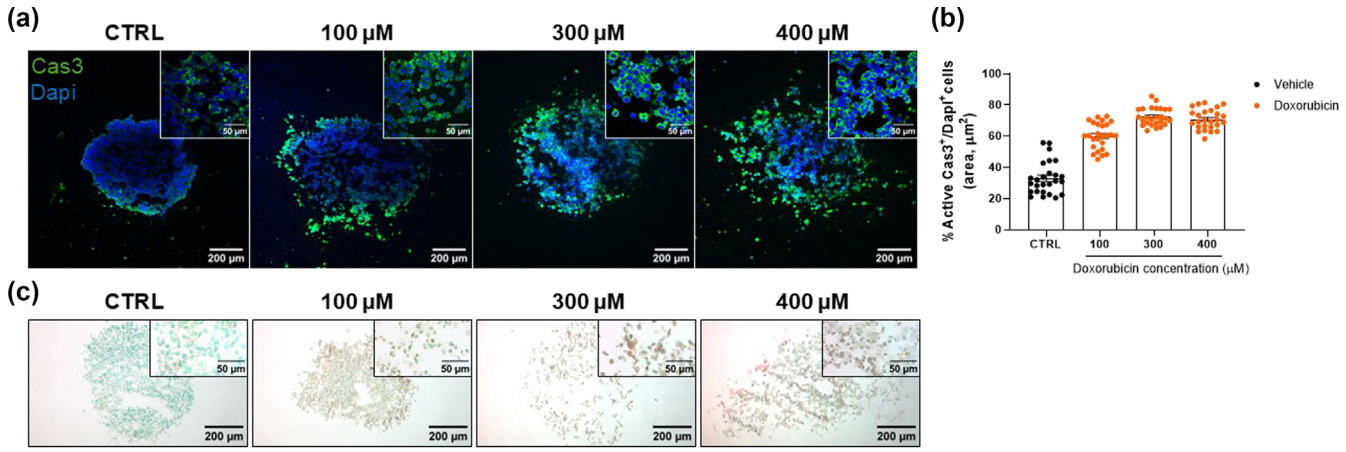

FIGURE 4 The high concentration of Doxorubicin (Dox) induces both mitochondrial and nuclear apoptosis. (a) Representative images and (b) relative quantification of active Caspase-3 (Cas3) staining in HBCSs. Enlarged areas are shown in the inserts within the merged images. Scale bars: 200 and 50 µm. Results are expressed as the percentage of active Cas3-positive cells (green) relative to the total number of DAPI-positive cells (blue) per area (μm^2) ± SEM. Each dot of the scatter dot plot represents the mean of four preselected areas per section of three spheroids per group from three independent experimental settings. An increase of 82.47%, 119.7% and 114.65% in Cas3 protein expression was detected in 100, 300 and 400 µM Dox-treated Human breast cancer spheroids (HBCSs) versus untreated controls (CTRL), respectively. (c) Representative images of HBCS cryosection stained by TUNEL assay and counterstained by 1% methyl green ($n = 3$ independent experimental settings, three spheroids per group for each experiment). Red/brown signal indicates apoptotic cells. Inserts within the merge pictures are enlarged areas. Scale bars: 200 and 50 µm.

3.4 | Overcoming Dox-resistance in breast cancer spheroids through induction of mitochondrial and nuclear apoptosis

To investigate whether high concentration of Dox-mediated viability defect is because of mitochondrial apoptosis, we stained spheroid cryosections with the antibody against cleaved caspase-3 (Cas3, green), an activated protease of the apoptotic cascade (Figure 4a). After 72 h exposure to 100–300–400 µM Dox, a markable non-concentration-dependent increase in the number of Cas3-positive cells was detected in MDAMB231/FB/EC spheroids (Figure 4b).

Given the absence of concentration-dependent changes in Cas3 levels with increasing Dox concentration, to verify nuclear apoptosis signalling, we checked cellular DNA fragmentation by TUNEL assay. Dox treatment triggered apoptosis, as indicated by an increasing number of TUNEL-positive cells in all Dox-treated spheroid conditions compared to vehicle group (Figure 4c). These data clearly show that a high concentration of Dox promotes mitochondrial dysfunction as well as DNA break to counteract the hypoxia-mediated chemoresistance.

3.5 | Correlation between ROS accumulation, PK2 release and Dox efficacy after overcoming resistance

Previous studies have demonstrated that Dox can cause the accumulation of ROS, which may contribute to the stabilisation of HIF-1α. This stabilisation is associated with genetic instability, metabolic reprogramming, malignant progression, metastasis and drug resistance (Movafagh et al., 2015). However, the inconsistent results observed with the use of antioxidants such as vitamins C and E, as well as β-carotene, to reduce oxidative damage, suggest that ROS may have a dual role in both promoting cancer cell proliferation and inducing apoptosis (Assi, 2017). In our breast cancer 3D model, we investigated the relationship between ROS levels and Dox-induced viability defects. We observed a clear dose-dependent increase in ROS levels in spheroids treated with 100–400 µM Dox, compared to untreated controls (Figure 5a). This ROS increase was not affected by HIF-1α inhibition (Figure 5b). Our results showed an inverse correlation between ROS levels and viability, suggesting that ROS may be crucial to Dox's effectiveness in overcoming chemotherapy resistance.

Cancer cells secrete a variety of factors collectively known as the secretome, including cytokines, chemokines, hormones and others, that may or may not contribute to cancer development and disease progression (Zahari et al., 2023). Secretome release can also be enhanced by chemotherapy. Among all secretome components, we focussed our attention on a chemokine-like protein, PK2, because of the presence of a HIF binding site at the *pk2* promoter (Désaubry et al., 2020). In addition, the up-regulation of proangiogenic cytokine PK2 expression has been described in many types of cancers (Vincenzi et al., 2023), and a growing body of evidence underscores the importance of PK2 as a biomarker in various diseases, including cancer (Yoshida et al., 2018).

Thus, we investigated whether a 72-h exposure to Dox affects the release of PK2 from HBCSs. Conditioned media were collected from both treated and untreated spheroids, and PK2 levels were measured using an ELISA assay. A notable increase in PK2 release was detected only in the conditioned medium of HBCSs treated with

14765381, 0, Downloaded from https://bpspubs.onlinelibrary.wiley.com/doi/10.1111/bph.70204 by Martina Vincenzi - University Di Roma La Sapienza , Wiley Online Library on [16/10/2025]. See the Terms and Conditions (https://onlinelibrary.wiley.com/terms-and-conditions) on Wiley Online Library for rules of use; OA articles are governed by the applicable Creative Commons License

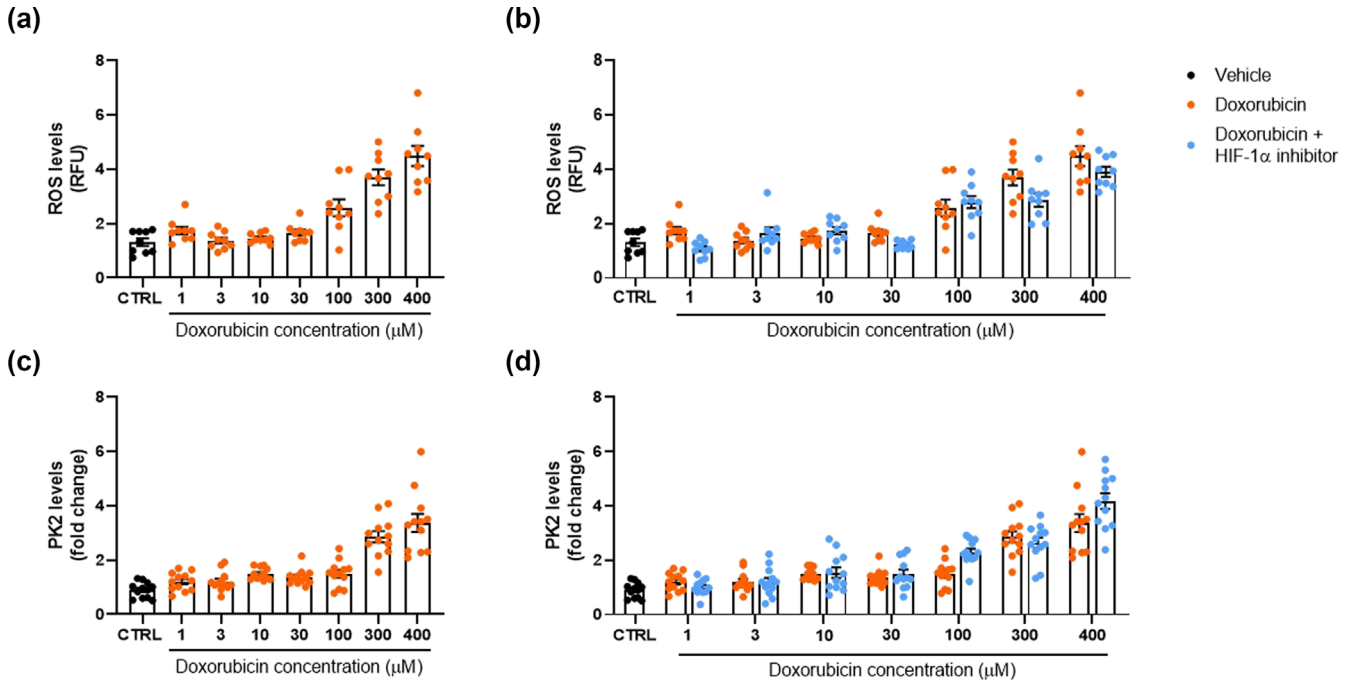

FIGURE 5 ROS-accumulation in breast cancer spheroids and PK2 release are associated with overcoming Doxorubicin (Dox) chemoresistance.(a, b) Quantification of ROS levels, expressed as Relative Fluorescence Units (RFU) ± SEM, in Dox-treated spheroids with or without HIF-1α inhibition. ($n = 3$ independent experimental settings, three spheroids per group for each experiment). A dose-dependent up-regulation of ROS levels was obtained at highest Dox concentrations (95.83%, 180.96% and 240.52% ROS increase in 100, 300 and 400 μM Dox-treated spheroids vs control [CTRL], respectively). The inhibition of HIF-1α did not affect Dox-mediated accumulation of ROS (111.91%, 117.91% and 196.81% ROS increase in 100, 300 and 400 μM Dox-treated + HIF-1α inhibitor groups vs CTRL, respectively). (b) $P < 0.0001$, 100–300–400 μM Dox + HIF-1α inhibitor groups versus vehicle group. (c) PK2 levels detected by ELISA in conditioned media from treated and untreated MDAMB231/FB/EC spheroids after 72 h of exposure to Dox (1–400 μM) or vehicle (CTRL). PK2 levels are expressed as individual values (fold-change) ± SEM of four spheroids per group from three independent experimental settings. A notable increase of PK2 levels was detected in the conditioned medium of HBCSs after 300 (218.5%) and 400 μM (275.38%) Dox treatment in comparisons with untreated controls. (d) PK2 levels in response to various Dox concentrations over 72 h in the presence of HIF-1α inhibition. The data presented are individual values (fold change) ± SEM. As expected, the HIF-1α inhibition did not display any effect on Dox-mediated PK2 release (193.74% and 365.18% increase of PK2 release in the conditioned medium of 300 and 400 μM Dox-treated + HIF-1α inhibitor groups vs CTRL, respectively). EC, Endothelial cell; FB, Fibroblast.

100 μM Dox. Indeed, a high PK2 release was observed after 300 and 400 μM Dox treatment of the spheroids compared to control (Figure 5c). Exposure to a HIF-1α inhibitor did not alter PK2 release by Dox (Figure 5d). Additionally, PK2 levels were inversely correlated with viability and ROS levels. These findings highlight the potential of PK2, as a hypoxia-independent biomarker of ROS-mediated Dox efficacy, in overcoming chemoresistance, and indicate its promise as a pharmacodynamic marker for Dox effectiveness.

4 | DISCUSSION

Breast and lung cancers are the most commonly diagnosed solid cancers and are among the leading causes of death worldwide after cardiovascular diseases (Sung et al., 2021). The recurrence of cancer after treatment with current therapies highlights the urgent need to explore the pathways involved in chemoresistance to identify potential alternative therapeutic strategies (Ncube et al., 2023). Dox is a widely used chemotherapy for early and advanced breast cancer. However, its effectiveness is limited by tumour resistance, the mechanisms of which remain poorly understood. In vitro studies using two-dimensional (2D) breast cancer cell models often lack clinical relevance. Over the past decades, the development of three-dimensional (3D) cultures has enabled researchers to address some of the limitations associated with traditional 2D cultures. Specifically, multicellular tumour spheroids have been widely recognised as effective tools for mimicking the in vivo response of cancer cells to treatment because of their physiological similarities to human solid tumours (Han et al., 2021; Nunes et al., 2019). In this context, we created a 3D tumour tissue model (HBCSs) that replicates the in vivo architecture of breast cancer and the anthracycline resistance commonly observed in vivo (Mattioli et al., 2023).

Several signalling pathways can influence the behaviour of breast cancer cells and contribute to the development of resistance to anthracyclines in a complex microenvironment. Several studies highlight the impact of tumour-microenvironment interactions on cellular

14765381, 0, Downloaded from https://bpspubs.onlinelibrary.wiley.com/doi/10.1111/bph.70204 by Martina Vincenzi - University Di Roma La Sapienza , Wiley Online Library on [16/10/2025]. See the Terms and Conditions (https://onlinelibrary.wiley.com/terms-and-conditions) on Wiley Online Library for rules of use; OA articles are governed by the applicable Creative Commons License

signalling, which may influence the tumour cell response to therapy in the clinical setting. In this study, the IC_{50} value of Dox for MDA-MB-231 co-cultured with ECs and FBs under 3D conditions was 150 ± 35 μM. In contrast, in a previous study using 3D spheroids consisting exclusively of MDA-MB-231 cells, an IC_{50} value of 636 ± 160 μM was obtained for Dox, values significantly higher than the IC_{50} values observed in 2D cultures (Lovitt et al., 2018). During our study, the involvement of the tumour microenvironment in the morphological organisation of 3D cancer models was determined by semi-thin analyses (Figure S1). Bi-culture spheroid models (cancer cells + FB) show a less organised structure compared to triple culture models (cancer cells + FB + EC), indicating that multicellular culture alters the structure and efficacy of Dox treatment.

Indeed, it is unlikely that the limited diffusion of Dox in 3D cells plays an important role in Dox resistance in HBCSs, as Dox can be detected at a concentration of 3 μM in the nuclei of 3D cell cultures (Figure S2). Instead, the slower growth rate of breast cancer cells in spheroid cultures could reduce the inhibitory effect of Dox. The cytotoxicity of anticancer drugs is generally less effective on slower dividing cells than on rapidly proliferating cells. Previous studies have also reported lower proliferation rates in MDA-MB-231 cells grown in 3D environments compared to 2D monolayers (Lovitt et al., 2018). These results suggest that breast cancer cells grown in 3D conditions exhibit greater Dox resistance than cells in 2D cultures, which is consistent with clinical observations.

Numerous studies have identified hypoxia as a key factor driving both intrinsic and acquired chemoresistance (Chen et al., 2020; Teicher, 1994; Vito et al., 2020). We hypothesised that the HBCSs might develop resistance as a result of Dox-induced hypoxia. Supporting this, inhibiting HIF-1α translocation increased the sensitivity of spheroids to Dox, as evidenced by further reduced viability, particularly in spheroids treated with 10, 30 and 100 μM Dox following HIF-1α inhibition. These findings suggest that Dox-induced hypoxia at the 10, 30 and 100 μM range diminishes its cytotoxic effectiveness via activating HIF1α-dependent prosurvival pathway, by upregulating genes involved in metabolism, invasion and anti-apoptosis, leading to chemoresistance. In this context, CD73 has been described as one of the key players in the HIF-driven immunosuppression, angiogenesis and drug resistance (Bach et al., 2023). Based on the evidence that some chemotherapeutic agents can induce a HIF-1α-dependent change in CD73 levels (Samanta et al., 2018), we demonstrated the increase in CD73 enzymatic activity in our breast cancer spheroids after 72 h of Dox exposure. However, HIF-1α-driven resistance at the high concentration of Dox was unaltered by HIF-1α inhibition, suggesting that additional apoptotic pathways are activated, which counteract resistance even in the presence of hypoxia. Indeed, sustained hypoxia causes caspase activation and autophagy-mediated apoptosis (Zaarour et al., 2021). We found that Dox induces a non-dose dependent mitochondrial Cas3 activation in the sustained hypoxic condition. Additionally, an increase in DNA double-strand breaks measured with the TUNEL in response to the Dox exposure indicated that the cytotoxicity of high concentrations (100–300 – 400 μM) of Dox was because of nuclear apoptosis. We had a similar observation in other 3D solid cancer models, such as MCF7/FB/EC spheroids and A549/FB/EC spheroids (*see* Figure S3–S5).

Previous studies have found that one of the main mechanisms of clinical treatment for many tumours is to stimulate an intracellular oxidative stress state to produce excessive intracellular ROS levels, causing death signals such as DNA damage and activation of apoptosis (Ma et al., 2014). Sustained ROS levels in drug-resistant HBCSs may drive the activation of the DNA damage response, likely increasing DNA double-strand breaks, as measured by the TUNEL assay, following high concentration of Dox exposure. These effects contribute to Dox's ability to overcome chemoresistance and enhance its therapeutic effectiveness, while acknowledging the ROS as an interplay between therapeutic mechanisms and potential cytotoxicity. However, as noted by Malla et al. (2021), physiological ROS levels can support breast cancer survival by promoting epithelial–mesenchymal transition, stem cell differentiation and metabolic reprogramming, whereas elevated ROS levels can be harmful, leading to apoptosis. Additionally, the role of ROS varies with cancer stage. Indeed, ROS can drive pro-oncogenic and pro-angiogenic signalling in early cancer stages, while contributing to tumour suppression in later stages (Assi, 2017). However, tumour cells can develop a set of complex and precise regulatory mechanisms (such as enhancing antioxidant capacity) during treatment and hence develop resistance.

A clear increase in PK2 release was detected in the spheroid-conditioned medium after 72 h of exposure to high concentrations of Dox. Surprisingly, this increase in PK2 levels was not affected by HIF-1α inhibition, suggesting that HIF-1 is not a regulator of the PK2 promoter in our model. The rise in PK2 levels was correlated with the percentage of surviving cells and ROS accumulation at higher Dox concentrations, highlighting PK2's potential as a predictive biomarker for Dox efficacy after overcoming resistance in HBCSs. Interestingly, PK2 did not act as a resistance-inducing factor, as its levels remained unchanged during resistance. Additionally, our findings suggest that PK2 could serve as a reliable pharmacodynamic biomarker for drug response in other 3D breast cancer and lung cancer models (*see* Figure S6). We are currently investigating whether the release of PK2 is a counter-mechanism against ROS accumulation and how the PK2 promoter is activated by Dox.

Importantly, PK2 has been particularly noted for its role in tumour growth and metastasis (Lattanzi et al., 2022). PK2 was shown to promote migration in breast cancer models of mice implanted with cell lines with different metastatic properties that developed Dox resistance (Morales et al., 2016). In breast cancer, high PK2 expression has been associated with advanced disease stages and poor patient outcomes, suggesting that PK2 levels could be used to monitor disease progression and response to treatment (Sasaki et al., 2018). Moreover, research has indicated that elevated blood levels of PK2 can serve as a predictive biomarker for cancer progression and patient prognosis (Yoshida et al., 2018).

Thus, our study showed the involvement of PK2 in key drug-efficacy processes across resistance braking conditions, making it a

14765381, 0, Downloaded from https://bpspubs.onlinelibrary.wiley.com/doi/10.1111/bph.70204 by Martina Vincenzi - University Di Roma La Sapienza , Wiley Online Library on [16/10/2025]. See the Terms and Conditions (https://onlinelibrary.wiley.com/terms-and-conditions) on Wiley Online Library for rules of use; OA articles are governed by the applicable Creative Commons License

promising target for diagnostic and therapeutic strategies aimed at improving patient outcomes.

5 | STUDY LIMITATION

A limitation of our study was the use of concentrations of Dox in the 3D system that were notably high and may not fully mimic the mechanisms observed in patients receiving clinical doses. However, several studies have demonstrated that the recommended cumulative lifetime dose of Dox for triple-negative breast cancer patients is 550 mg m^{-2} of body surface area. Similarly, research has shown that intracellular Dox concentrations can be approximately 230 times higher than the exposure levels following treatment with free Dox (Kullenberg et al., 2021). Whether serum Dox concentrations accurately reflect the accumulation of Dox in cancer, and whether 3D breast cancer models fully reflect chemoresistance of human breast cancer remain controversial. Despite these limitations, our findings highlight the potential of PK2 as a biomarker for Dox efficacy, warranting further exploration in clinical studies.

To better understand the involvement of the tumour microenvironment in chemoresistance, future studies should analyse multiculture spheroid models incorporating cancer cells, FBs, ECs, and macrophages. Additionally, this study did not evaluate other mechanisms contributing to Dox resistance. Changes in the expression of other genes and the release of alternative cytokines should also be investigated. These efforts will deepen our understanding of the factors influencing Dox efficacy and resistance, paving the way for more effective therapeutic strategies.

6 | CONCLUSION

Doxorubicin (Dox) is one of the most widely used chemotherapy agents for the treatment of breast cancer. However, the development of Dox resistance limits the long-term treatment benefits in patients with breast cancer. The identification of a biomarker for hypoxia-mediated chemoresistance or effective drug response after overcoming the resistance could be useful to predict treatment effect and enable the development of new adjuvant anticancer drugs. The multicellular spheroid model appears to be an effective tool for studying the mechanisms of cell interactions, drug response and chemoresistance. We thus developed a 3D breast cancer model that mimics the architecture of a solid tumour by aggregating cancer cells, FBs and ECs. This model successfully replicates the development of hypoxia-induced resistance to Dox, a phenomenon known to contribute to cancer recurrence in vivo. Although further studies are needed to validate our findings in clinic, we propose, for the first time, PK2 as a biomarker for overcoming resistance. Assessing PK2 release could be a simple method to predict anthracycline efficacy at high concentrations. Conversely, patients with low PK2 levels might benefit more from alternative treatment strategies after developing resistance to Dox, rather than enduring the potentially ineffective and toxic side effects of continued chemotherapy. Our findings demonstrate compelling evidence that PK2 holds a significant promise as a biomarker for overcoming chemoresistance in breast cancer, paving the way for more effective therapies and substantially enhancing patient survival outcomes.

AUTHOR CONTRIBUTIONS

Martina Vincenzi: Data curation (equal); formal analysis (equal); investigation (equal); methodology (equal); visualisation (equal); writing—original draft preparation and writing—review and editing (equal). **Amin Kremic**: data curation and investigation (equal). **Nathalie N. Tscheiller**: data curation; investigation and methodology (supporting). **Po-Yen Hsu**: data curation; investigation and writing—original draft preparation. **Michael W.Y. Chan**: validation; writing—original draft preparation and writing—review and editing (supporting). **Roberta Lattanzi**: validation (supporting) and writing—original draft preparation. **Canan G. Nebigil**: conceptualisation (lead); data curation (equal); funding acquisition (lead); project administration (equal); supervision (lead); validation (equal); visualisation (equal); writing—original draft preparation (equal) and writing—review and editing (lead).

ACKNOWLEDGEMENTS

This study was supported by grants Foundation de France (R20085MM and R023044MM), and MV was financially supported by Sapienza University of Rome doctoral fellowship and fellowship of Italian Society of Pharmacology (SIF); AK and PYH were supported by Foundation France and Agence Nationale de la Recherche grants (ANR0005). We thank IGBMC, Illkirch for providing cancer cell lines. We would like to thank Herve Gegout and Dr Gilles Kauffenstein for the technical support.

CONFLICT OF INTEREST STATEMENT

The authors declare that they have no known competing financial interests or personal relationships that could have appeared to influence the work reported in this paper.

DATA AVAILABILITY STATEMENT

The data that support the findings of this study are available from the corresponding author upon reasonable request.

DECLARATION OF TRANSPARENCY AND SCIENTIFIC RIGOUR

This declaration confirms that the paper complies with the principles of transparent reporting and scientific rigour of preclinical research, as outlined in the *BJP* guidelines for study design, data analysis, and experimentation, and as endorsed by funding agencies, publishers, and research-supporting organizations.

REFERENCES

Aas, T., Børresen, A. L., Geisler, S., Smith-Sørensen, B., Johnsen, H., Varhaug, J. E., Akslen, L. A., & Lønning, P. E. (1996). Specific P53 mutations are associated with de novo resistance to doxorubicin in breast

14765381, 0, Downloaded from https://bpspubs.onlinelibrary.wiley.com/doi/10.1111/bph.70204 by Martina Vincenzi - University Di Roma La Sapienza , Wiley Online Library on [16/10/2025]. See the Terms and Conditions (https://onlinelibrary.wiley.com/terms-and-conditions) on Wiley Online Library for rules of use; OA articles are governed by the applicable Creative Commons License

cancer patients. *Nature Medicine*, *2*(7), 811–814. https://doi.org/10.1038/nm0796-811

Alexander, S. P. H., Christopoulos, A., Davenport, A. P., Kelly, E., Mathie, A. A., Peters, J. A., Veale, E. L., Armstrong, J. F., Faccenda, E., Harding, S. D., Davies, J. A., Abbracchio, M. P., Abraham, G., Agoulnik, A., Alexander, W., Al-Hosaini, K., Bäck, M., Baker, J. G., Barnes, N. M., … Ye, R. D. (2023). The Concise Guide to PHARMACOLOGY 2023/24: G protein-coupled receptors. *British Journal of Pharmacology*, *180*, S23–S144. https://doi.org/10.1111/bph.16177

Alexander, S. P. H., Fabbro, D., Kelly, E., Mathie, A. A., Peters, J. A., Veale, E. L., Armstrong, J. F., Faccenda, E., Harding, S. D., Davies, J. A., Amarosi, L., Anderson, C. M. H., Beart, P. M., Broer, S., Dawson, P. A., Gyimesi, G., Hagenbuch, B., Hammond, J. R., Hancox, J. C., … Verri, T. (2023). The Concise Guide to PHARMACOLOGY 2023/24: Transporters. *British Journal of Pharmacology*, *180*, S374–S469. https://doi.org/10.1111/bph.16182

Alexander, S. P. H., Fabbro, D., Kelly, E., Mathie, A. A., Peters, J. A., Veale, E. L., Armstrong, J. F., Faccenda, E., Harding, S. D., Davies, J. A., Annett, S., Boison, D., Burns, K. E., Dessauer, C., Gertsch, J., Helsby, N. A., Izzo, A. A., Ostrom, R., Papapetropoulos, A., … Wong, S. S. (2023). The concise guide to PHARMACOLOGY 2023/24: Enzymes. *British Journal of Pharmacology*, *180*, S289–S373. https://doi.org/10.1111/bph.16181

Alexander, S. P. H., Kelly, E., Mathie, A. A., Peters, J. A., Veale, E. L., Armstrong, J. F., Buneman, O. P., Faccenda, E., Harding, S. D., Spedding, M., Cidlowski, J. A., Fabbro, D., Davenport, A. P., Striessnig, J., Davies, J. A., Ahlers-Dannen, K. E., Alqinyah, M., Arumugam, T. V., Bodle, C., … Zolghadri, Y. (2023). The Concise Guide to PHARMACOLOGY 2023/24: Introduction and Other Protein Targets. *British Journal of Pharmacology*, *180*, S1–S22. https://doi.org/10.1111/bph.16176

Assi, M. (2017). The differential role of reactive oxygen species in early and late stages of cancer. *American Journal of Physiology. Regulatory, Integrative and Comparative Physiology*, *313*(6), R646–r653. https://doi.org/10.1152/ajpregu.00247.2017

Bach, N., Winzer, R., Tolosa, E., Fiedler, W., & Brauneck, F. (2023). The clinical significance of CD73 in cancer. *International Journal of Molecular Sciences*, *24*(14), 11759. https://doi.org/10.3390/ijms241411759

Badinloo, M., & Esmaeili-Mahani, S. (2014). Phosphatidylinositol 3-kinases inhibitor LY294002 potentiates the cytotoxic effects of doxorubicin, vincristine, and etoposide in a panel of cancer cell lines. *Fundamental & Clinical Pharmacology*, *28*(4), 414–422. https://doi.org/10.1111/fcp.12043

Bissell, M. J., & Radisky, D. (2001). Putting tumours in context. *Nature Reviews. Cancer*, *1*(1), 46–54. https://doi.org/10.1038/35094059

Bouleftour, W., Rowinski, E., Louati, S., Sotton, S., Wozny, A. S., Moreno-Acosta, P., Mery, B., Rodriguez-Lafrasse, C., & Magne, N. (2021). A review of the role of hypoxia in radioresistance in cancer therapy. *Medical Science Monitor*, *27*, e934116. https://doi.org/10.12659/msm.934116

Braun, N., Sévigny, J., Robson, S. C., Enjyoji, K., Guckelberger, O., Hammer, K., Di Virgilio, F., & Zimmermann, H. (2000). Assignment of ecto-nucleoside triphosphate diphosphohydrolase-1/cd39 expression to microglia and vasculature of the brain. *European Journal of Neuroscience*, *12*(12), 4357–4366. https://doi.org/10.1111/j.1460-9568.2000.01342.x

Bueb, J. L., Gallois, A., Schneider, J. C., Parini, J. P., & Tschirhart, E. (1995). A double-labelling fluorescent assay for concomitant measurements of [Ca2+]i and O2 production in human macrophages. *Biochimica et Biophysica Acta*, *1244*(1), 79–84. https://doi.org/10.1016/0304-4165(94)00198-7

Cao, Y., Eble, J. M., Moon, E., Yuan, H., Weitzel, D. H., Landon, C. D., Yu-Chih Nien, C., Hanna, G., Rich, J. N., Provenzale, J. M., & Dewhirst, M. W. (2013). Tumor cells upregulate normoxic HIF-1α in response to doxorubicin. *Cancer Research*, *73*(20), 6230–6242. https://doi.org/10.1158/0008-5472.Can-12-1345

Chen, N.-N., Ma, X.-D., Miao, Z., Zhang, X.-M., Han, B.-Y., Almaamari, A. A., Huang, J.-M., Chen, X.-Y., Liu, Y.-J., & Su, S.-W. (2023). Doxorubicin resistance in breast cancer is mediated via the activation of FABP5/PPARγ and CaMKII signaling pathway. *Frontiers in Pharmacology*, *14*, 1150861. https://doi.org/10.3389/fphar.2023.1150861

Chen, P. S., Chiu, W. T., Hsu, P. L., Lin, S. C., Peng, I. C., Wang, C. Y., & Tsai, S. J. (2020). Pathophysiological implications of hypoxia in human diseases. *Journal of Biomedical Science*, *27*(1), 63. https://doi.org/10.1186/s12929-020-00658-7

Christowitz, C., Davis, T., Isaacs, A., van Niekerk, G., Hattingh, S., & Engelbrecht, A. M. (2019). Mechanisms of doxorubicin-induced drug resistance and drug resistant tumour growth in a murine breast tumour model. *BMC Cancer*, *19*(1), 757. https://doi.org/10.1186/s12885-019-5939-z

Curtis, M. J., Alexander, S. P. H., Cortese-Krott, M., Kendall, D. A., Martemyanov, K. A., Mauro, C., Panettieri, R. A. Jr., Papapetropoulos, A., Patel, H. H., Santo, E. E., Schulz, R., Stefanska, B., Stephens, G. J., Teixeira, M. M., Vergnolle, N., Wang, X., & Ferdinandy, P. (2025). Guidance on the planning and reporting of experimental design and analysis. *British Journal of Pharmacology*, *182*(7), 1413–1415. https://doi.org/10.1111/bph.17441

Désaubry, L., Kanthasamy, A. G., & Nebigil, C. G. (2020). Prokineticin signaling in heart-brain developmental axis: Therapeutic options for heart and brain injuries. *Pharmacological Research*, *160*, 105190. https://doi.org/10.1016/j.phrs.2020.105190

Doublier, S., Belisario, D. C., Polimeni, M., Annaratone, L., Riganti, C., Allia, E., Ghigo, D., Bosia, A., & Sapino, A. (2012). HIF-1 activation induces doxorubicin resistance in MCF7 3-D spheroids via P-glycoprotein expression: A potential model of the chemo-resistance of invasive micropapillary carcinoma of the breast. *BMC Cancer*, *12*(4), 4. https://doi.org/10.1186/1471-2407-12-4

Dulf, P. L., Mocan, M., Coadă, C. A., Dulf, D. V., Moldovan, R., Baldea, I., Farcas, A. D., Blendea, D., & Filip, A. G. (2023). Doxorubicin-induced acute cardiotoxicity is associated with increased oxidative stress, autophagy, and inflammation in a murine model. *Naunyn-Schmiedeberg's Archives of Pharmacology*, *396*(6), 1105–1115. https://doi.org/10.1007/s00210-023-02382-z

Fan, P., Zhang, N., Candi, E., Agostini, M., Piacentini, M., Shi, Y., Huang, Y., & Melino, G. (2023). Alleviating hypoxia to improve cancer immunotherapy. *Oncogene*, *42*(49), 3591–3604. https://doi.org/10.1038/s41388-023-02869-2

Fourie, C., du Plessis, M., Mills, J., & Engelbrecht, A. M. (2022). The effect of HIF-1α inhibition in breast cancer cells prior to doxorubicin treatment under conditions of normoxia and hypoxia. *Experimental Cell Research*, *419*(2), 113334. https://doi.org/10.1016/j.yexcr.2022.113334

Gasser, A., Chen, Y. W., Audebrand, A., Daglayan, A., Charavin, M., Escoubet, B., Karpov, P., Tetko, I., Chan, M. W. Y., Cardinale, D., Désaubry, L., & Nebigil, C. G. (2019). Prokineticin receptor-1 signaling inhibits dose- and time-dependent anthracycline-induced cardiovascular toxicity via myocardial and vascular protection. *JACC CardioOncol*, *1*(1), 84–102. https://doi.org/10.1016/j.jaccao.2019.06.003

Haibe, Y., Kreidieh, M., El Hajj, H., Khalifeh, I., Mukherji, D., Temraz, S., & Shamseddine, A. (2020). Resistance mechanisms to anti-angiogenic therapies in cancer. *Frontiers in Oncology*, *10*, 221. https://doi.org/10.3389/fonc.2020.00221

Han, S. J., Kwon, S., & Kim, K. S. (2021). Challenges of applying multicellular tumor spheroids in preclinical phase. *Cancer Cell International*, *21*(1), 152. https://doi.org/10.1186/s12935-021-01853-8

Hernandez-Aya, L. F., & Gonzalez-Angulo, A. M. (2013). Adjuvant systemic therapies in breast cancer. *The Surgical Clinics of North America*, *93*(2), 473–491. https://doi.org/10.1016/j.suc.2012.12.002

14765381, 0, Downloaded from https://bpspubs.onlinelibrary.wiley.com/doi/10.1111/bph.70204 by Martina Vincenzi - University Di Roma La Sapienza , Wiley Online Library on [16/10/2025]. See the Terms and Conditions (https://onlinelibrary.wiley.com/terms-and-conditions) on Wiley Online Library for rules of use; OA articles are governed by the applicable Creative Commons License

Kciuk, M., Gielecińska, A., Mujwar, S., Kołat, D., Kałuzińska-Kołat, Ż., Celik, I., & Kontek, R. (2023). Doxorubicin—An agent with multiple mechanisms of anticancer activity. *Cells*, *12*(4), 659. https://doi.org/10.3390/cells12040659

Kullenberg, F., Degerstedt, O., Calitz, C., Pavlovic, N., Balgoma, D., Grasjo, J., Sjogren, E., Hedeland, M., Heindryckx, F., & Lennernas, H. (2021). In vitro cell toxicity and intracellular uptake of doxorubicin exposed as a solution or liposomes: Implications for treatment of hepatocellular carcinoma. *Cells*, *10*(7), 1717. https://doi.org/10.3390/cells10071717

Lattanzi, R., Severini, C., & Miele, R. (2022). Prokineticin 2 in cancer-related inflammation. *Cancer Letters*, *546*, 215838. https://doi.org/10.1016/j.canlet.2022.215838

Lee, J. W., Ko, J., Ju, C., & Eltzschig, H. K. (2019). Hypoxia signaling in human diseases and therapeutic targets. *Experimental & Molecular Medicine*, *51*(6), 1–13. https://doi.org/10.1038/s12276-019-0235-1

Li, J., Shi, M., Cao, Y., Yuan, W., Pang, T., Li, B., Sun, Z., Chen, L., & Zhao, R. C. (2006). Knockdown of hypoxia-inducible factor-1alpha in breast carcinoma MCF-7 cells results in reduced tumor growth and increased sensitivity to methotrexate. *Biochemical and Biophysical Research Communications*, *342*(4), 1341–1351. https://doi.org/10.1016/j.bbrc.2006.02.094

Liu, Q., Guan, C., Liu, C., Li, H., Wu, J., & Sun, C. (2022). Targeting hypoxia-inducible factor-1alpha: A new strategy for triple-negative breast cancer therapy. *Biomedicine & Pharmacotherapy*, *156*, 113861. https://doi.org/10.1016/j.biopha.2022.113861

Lovitt, C. J., Shelper, T. B., & Avery, V. M. (2018). Doxorubicin resistance in breast cancer cells is mediated by extracellular matrix proteins. *BMC Cancer*, *18*(1), 41. https://doi.org/10.1186/s12885-017-3953-6

Ma, Y., Chapman, J., Levine, M., Polireddy, K., Drisko, J., & Chen, Q. (2014). High-dose parenteral ascorbate enhanced chemosensitivity of ovarian cancer and reduced toxicity of chemotherapy. *Science Translational Medicine*, *6*(222), 222ra218. https://doi.org/10.1126/scitranslmed.3007154

Malla, R., Surepalli, N., Farran, B., Malhotra, S. V., & Nagaraju, G. P. (2021). Reactive oxygen species (ROS): Critical roles in breast tumor microenvironment. *Critical Reviews in Oncology/Hematology*, *160*, 103285. https://doi.org/10.1016/j.critrevonc.2021.103285

Mattioli, R., Ilari, A., Colotti, B., Mosca, L., Fazi, F., & Colotti, G. (2023). Doxorubicin and other anthracyclines in cancers: Activity, chemoresistance and its overcoming. *Molecular Aspects of Medicine*, *93*, 101205. https://doi.org/10.1016/j.mam.2023.101205

McAleese, C. E., Choudhury, C., Butcher, N. J., & Minchin, R. F. (2021). Hypoxia-mediated drug resistance in breast cancers. *Cancer Letters*, *502*, 189–199. https://doi.org/10.1016/j.canlet.2020.11.045

Mechetner, E., Kyshtoobayeva, A., Zonis, S., Kim, H., Stroup, R., Garcia, R., Parker, R. J., & Fruehauf, J. P. (1998). Levels of multidrug resistance (MDR1) P-glycoprotein expression by human breast cancer correlate with in vitro resistance to taxol and doxorubicin. *Clinical Cancer Research*, *4*(2), 389–398.

Mehta, G., Hsiao, A. Y., Ingram, M., Luker, G. D., & Takayama, S. (2012). Opportunities and challenges for use of tumor spheroids as models to test drug delivery and efficacy. *Journal of Controlled Release*, *164*(2), 192–204. https://doi.org/10.1016/j.jconrel.2012.04.045

Morales, A., Morimoto, S., Vilchis, F., Taniyama, N., Bautista, C. J., Robles, C., & Bargallo, E. (2016). Molecular expression of vascular endothelial growth factor, prokineticin receptor-1 and other biomarkers in infiltrating canalicular carcinoma of the breast. *Oncology Letters*, *12*(4), 2720–2727. https://doi.org/10.3892/ol.2016.4961

Movafagh, S., Crook, S., & Vo, K. (2015). Regulation of hypoxia-inducible factor-1a by reactive oxygen species: New developments in an old debate. *Journal of Cellular Biochemistry*, *116*(5), 696–703. https://doi.org/10.1002/jcb.25074

Ncube, K. N., Jurgens, T., Steenkamp, V., Cromarty, A. D., van den Bout, I., & Cordier, W. (2023). Comparative evaluation of the cytotoxicity of doxorubicin in BT-20 triple-negative breast carcinoma monolayer and spheroid cultures. *Biomedicine*, *11*(5), 1484. https://doi.org/10.3390/biomedicines11051484

Nebigil, C. G., & Désaubry, L. (2018). Updates in anthracycline-mediated cardiotoxicity. *Frontiers in Pharmacology*, *9*, 1262. https://doi.org/10.3389/fphar.2018.01262

Nunes, A. S., Barros, A. S., Costa, E. C., Moreira, A. F., & Correia, I. J. (2019). 3D tumor spheroids as in vitro models to mimic in vivo human solid tumors resistance to therapeutic drugs. *Biotechnology and Bioengineering*, *116*(1), 206–226. https://doi.org/10.1002/bit.26845

Pan, X., Hong, X., Li, S., Meng, P., & Xiao, F. (2021). METTL3 promotes adriamycin resistance in MCF-7 breast cancer cells by accelerating pri-microRNA-221-3p maturation in a m6A-dependent manner. *Experimental & Molecular Medicine*, *53*(1), 91–102. https://doi.org/10.1038/s12276-020-00510-w

Ponnusamy, L., Mahalingaiah, P. K. S., & Singh, K. P. (2017). Treatment schedule and estrogen receptor-status influence acquisition of doxorubicin resistance in breast cancer cells. *European Journal of Pharmaceutical Sciences*, *104*, 424–433. https://doi.org/10.1016/j.ejps.2017.04.020

Saitoh, A., & Nagase, H. (2018). Delta opioid receptor (DOR) ligands and pharmacology: Development of indolo- and quinolinomorphinan derivatives based on the message-address concept. In E. Jutkiewicz (Ed.), *Delta opioid receptor pharmacology and therapeutic applications. Handbook of Experimental Pharmacology* (Vol. 247). Springer. https://doi.org/10.1007/164_2016_18

Samanta, D., Park, Y., Ni, X., Li, H., Zahnow, C. A., Gabrielson, E., Pan, F., & Semenza, G. L. (2018). Chemotherapy induces enrichment of CD47(+)/CD73(+)/PDL1(+) immune evasive triple-negative breast cancer cells. *Proceedings of the National Academy of Sciences of the United States of America*, *115*(6), E1239–e1248. https://doi.org/10.1073/pnas.1718197115

Sasaki, S., Baba, T., Muranaka, H., Tanabe, Y., Takahashi, C., Matsugo, S., & Mukaida, N. (2018). Involvement of prokineticin 2-expressing neutrophil infiltration in 5-fluorouracil-induced aggravation of breast cancer metastasis to lung. *Molecular Cancer Therapeutics*, *17*(7), 1515–1525. https://doi.org/10.1158/1535-7163.Mct-17-0845

Semenza, G. L. (2016). The hypoxic tumor microenvironment: A driving force for breast cancer progression. *Biochimica et Biophysica Acta*, *1863*(3), 382–391. https://doi.org/10.1016/j.bbamcr.2015.05.036

Shi, Y., Bieerkehazhi, S., & Ma, H. (2018). Next-generation proteasome inhibitor oprozomib enhances sensitivity to doxorubicin in triple-negative breast cancer cells. *International Journal of Clinical and Experimental Pathology*, *11*(5), 2347–2355.

Shojaei, F., Wu, X., Qu, X., Kowanetz, M., Yu, L., Tan, M., Meng, Y. G., & Ferrara, N. (2009). G-CSF-initiated myeloid cell mobilization and angiogenesis mediate tumor refractoriness to anti-VEGF therapy in mouse models. *Proceedings of the National Academy of Sciences of the United States of America*, *106*(16), 6742–6747. https://doi.org/10.1073/pnas.0902280106

Shojaei, F., Wu, X., Zhong, C., Yu, L., Liang, X. H., Yao, J., Blanchard, D., Bais, C., Peale, F. V., van Bruggen, N., Ho, C., Ross, J., Tan, M., Carano, R. A., Meng, Y. G., & Ferrara, N. (2007). Bv8 regulates myeloid-cell-dependent tumour angiogenesis. *Nature*, *450*(7171), 825–831. https://doi.org/10.1038/nature06348

Song, X., Liu, X., Chi, W., Liu, Y., Wei, L., Wang, X., & Yu, J. (2006). Hypoxia-induced resistance to cisplatin and doxorubicin in non-small cell lung cancer is inhibited by silencing of HIF-1alpha gene. *Cancer Chemotherapy and Pharmacology*, *58*(6), 776–784. https://doi.org/10.1007/s00280-006-0224-7

Sung, H., Ferlay, J., Siegel, R. L., Laversanne, M., Soerjomataram, I., Jemal, A., & Bray, F. (2021). Global Cancer Statistics 2020: GLOBOCAN Estimates of Incidence and Mortality Worldwide for 36 Cancers in 185 Countries. *CA: a Cancer Journal for Clinicians*, *71*(3), 209–249. https://doi.org/10.3322/caac.21660

14765381, 0, Downloaded from https://bpspubs.onlinelibrary.wiley.com/doi/10.1111/bph.70204 by Martina Vincenzi - University Di Roma La Sapienza , Wiley Online Library on [16/10/2025]. See the Terms and Conditions (https://onlinelibrary.wiley.com/terms-and-conditions) on Wiley Online Library for rules of use; OA articles are governed by the applicable Creative Commons License

Synnestvedt, K., Furuta, G. T., Comerford, K. M., Louis, N., Karhausen, J., Eltzschig, H. K., Hansen, K. R., Thompson, L. F., & Colgan, S. P. (2002). Ecto-5′-nucleotidase (CD73) regulation by hypoxia-inducible factor-1 mediates permeability changes in intestinal epithelia. *The Journal of Clinical Investigation*, *110*(7), 993–1002. https://doi.org/10.1172/jci15337

Teicher, B. A. (1994). Hypoxia and drug resistance. *Cancer Metastasis Reviews*, *13*(2), 139–168. https://doi.org/10.1007/bf00689633

Vincenzi, M., Kremić, A., Jouve, A., Lattanzi, R., Miele, R., Benharouga, M., Alfaidy, N., Migrenne-Li, S., Kanthasamy, A. G., Porcionatto, M., Ferrara, N., Tetko, I. V., Désaubry, L., & Nebigil, C. G. (2023). Therapeutic potential of targeting prokineticin receptors in diseases. *Pharmacological Reviews*, *75*(6), 1167–1199. https://doi.org/10.1124/pharmrev.122.000801

Vito, A., El-Sayes, N., & Mossman, K. (2020). Hypoxia-driven immune escape in the tumor microenvironment. *Cells*, *9*(4), 992. https://doi.org/10.3390/cells9040992

Wachstein, M., & Meisel, E. (1957). Histochemistry of hepatic phosphatases of a physiologic pH; with special reference to the demonstration of bile canaliculi. *American Journal of Clinical Pathology*, *27*(1), 13–23. https://doi.org/10.1093/ajcp/27.1.13

Wang, S., Konorev, E. A., Kotamraju, S., Joseph, J., Kalivendi, S., & Kalyanaraman, B. (2004). Doxorubicin induces apoptosis in normal and tumor cells via distinctly different mechanisms. Intermediacy of H_2O_2- and p53-dependent pathways. *The Journal of Biological Chemistry*, *279*(24), 25535–25543. https://doi.org/10.1074/jbc.M400944200

Wartenberg, M., Ling, F. C., Müschen, M., Klein, F., Acker, H., Gassmann, M., Petrat, K., Pütz, V., Hescheler, J., & Sauer, H. (2003). Regulation of the multidrug resistance transporter P-glycoprotein in multicellular tumor spheroids by hypoxia-inducible factor-1 and reactive oxygen species. *The FASEB Journal*, *17*(3), 1–22. https://doi.org/10.1096/fj.02-0358fje

Yakavets, I., Francois, A., Benoit, A., Merlin, J. L., Bezdetnaya, L., & Vogin, G. (2020). Advanced co-culture 3D breast cancer model for investigation of fibrosis induced by external stimuli: optimization study. *Scientific Reports*, *10*(1), 21273. https://doi.org/10.1038/s41598-020-78087-7

Yeh, P. Y., Chuang, S. E., Yeh, K. H., Song, Y. C., Chang, L. L., & Cheng, A. L. (2004). Phosphorylation of p53 on Thr55 by ERK2 is necessary for doxorubicin-induced p53 activation and cell death. *Oncogene*, *23*(20), 3580–3588. https://doi.org/10.1038/sj.onc.1207426

Yoshida, Y., Goi, T., Kurebayashi, H., Morikawa, M., Hirono, Y., & Katayama, K. (2018). Prokineticin 2 expression as a novel prognostic biomarker for human colorectal cancer. *Oncotarget*, *9*(53), 30079–30091. https://doi.org/10.18632/oncotarget.25706

Yu, Y., Dai, M., Xu, W., Chen, S., & Lu, Q. (2021). Close to real: Large-volume 3D cell spheroids on a superamphiphobic surface. *Advanced Materials Interfaces*, *8*(9), 2100039. https://doi.org/10.1002/admi.202100039

Zaarour, R. F., Azakir, B., Hajam, E. Y., Nawafleh, H., Zeinelabdin, N. A., Engelsen, A. S. T., Thiery, J., Jamora, C., & Chouaib, S. (2021). Role of hypoxia-mediated autophagy in tumor cell death and survival. *Cancers (Basel)*, *13*(3), 533. https://doi.org/10.3390/cancers13030533

Zahari, S., Syafruddin, S. E., & Mohtar, M. A. (2023). Impact of the cancer cell secretome in driving breast cancer progression. *Cancers*, *15*(9), 2653. https://doi.org/10.3390/cancers15092653

Zhang, L., Yu, D., Hicklin, D. J., Hannay, J. A., Ellis, L. M., & Pollock, R. E. (2002). Combined anti-fetal liver kinase 1 monoclonal antibody and continuous low-dose doxorubicin inhibits angiogenesis and growth of human soft tissue sarcoma xenografts by induction of endothelial cell apoptosis. *Cancer Research*, *62*(7), 2034–2042.

Zhao, J., Zhang, H., Liu, Y., Lu, G., Wang, Z., Mo, Q., Wang, G., Shen, Y., & Jiao, L. (2024). HIF-1α knockdown suppresses breast cancer metastasis via epithelial mesenchymal transition abrogation. *Heliyon*, *10*(19), e37900. https://doi.org/10.1016/j.heliyon.2024.e37900

Zhou, Y., Liu, T., Wu, Q., Wang, H., & Sun, Y. (2023). Baohuoside I inhibits resistance to cisplatin in ovarian cancer cells by suppressing autophagy via downregulating HIF-1α/ATG5 axis. *Molecular Carcinogenesis*, *62*(10), 1474–1486. https://doi.org/10.1002/mc.23590

SUPPORTING INFORMATION

Additional supporting information can be found online in the Supporting Information section at the end of this article.

How to cite this article: Vincenzi, M., Kremic, A., Tscheiller, N. N., Hsu, P.-Y., Chan, M. W. Y., Lattanzi, R., & Nebigil, C. G. (2025). Identification of prokineticin-2 as potential pharmacodynamic biomarker for overcoming doxorubicin resistance in multicellular breast cancer spheroids. *British Journal of Pharmacology*, 1–14. https://doi.org/10.1111/bph.70204

14765381, 0, Downloaded from https://bpspubs.onlinelibrary.wiley.com/doi/10.1111/bph.70204 by Martina Vincenzi - University Di Roma La Sapienza , Wiley Online Library on [16/10/2025]. See the Terms and Conditions (https://onlinelibrary.wiley.com/terms-and-conditions) on Wiley Online Library for rules of use; OA articles are governed by the applicable Creative Commons License